

miR-146b-5p activation of hepatic stellate cells contributes to the progression of fibrosis by directly targeting HIPK1

JUNFENG XIE^{1,2*}, NA CHENG^{3*}, ZHANCHAO HUANG¹, XU SHU¹ and TIANXIN XIANG¹

¹Department of Hospital Infection Control, The First Affiliated Hospital of Nanchang University, Nanchang, Jiangxi 330000;

²Department of Gastroenterology, The People's Hospital of Ganzhou City, Ganzhou, Jiangxi 341000; ³Department of Infectious Disease, The First Affiliated Hospital of Nanchang University, Nanchang, Jiangxi 330000, P.R. China

Received July 22, 2021; Accepted March 7, 2022

DOI: 10.3892/etm.2022.11474

Abstract. The present study aimed to explore the biological functions of microRNA (miR)-146b-5p and homeodomain interacting protein kinase 1 (HIPK1) in the progression of hepatic fibrosis (HF) and to identify the underlying mechanism. A rat HF model was established by administering a subcutaneous injection of carbon tetrachloride (CCl₄). Relative levels of miR-146b-5p and HIPK1 in fibrotic rat liver tissues and the rat hepatic stellate cell (HSC) line HSC-T6 were measured by quantitative reverse transcription PCR, western blotting and immunohistochemistry. Following activation of HSC-T6 cells by lipopolysaccharide (LPS) induction, cell viability was examined by MTT assay. Transfection of miR-146b-5p mimic or inhibitor into HSC-T6 cells was performed, with the aim to identify the influence of miR-146b-5p on HSC-T6 cell behavior. The targeting relationship between miR-146b-5p and HIPK1 was predicted by TargetScan 7.2 and StarBase 3.0 and it was later verified by a dual-luciferase reporter assay. Through lentivirus transfection, the biological function of HIPK1 in regulating the progression of HF and the underlying mechanism were investigated. The results showed that miR-146b-5p was upregulated in liver tissues of rats with HF and activated HSC-T6 cells, while HIPK1 was downregulated in liver tissues of rats with HF and activated HSC-T6 cells. miR-146b-5p was able to upregulate the activation markers of LPS-induced HSC-T6 cells, upregulate COL1A1 and TGF- β , increase cell viability and contribute to fibrosis progression. HIPK1 was validated as the direct target of miR-146b-5p and its overexpression could effectively reduce the effect of

miR-146b-5p in contribution to the progression of HF. In conclusion, miR-146b-5p was significantly upregulated during the progression of HF. By targeting and downregulating HIPK1, miR-146b-5p could significantly activate HSCs, upregulate COL1A1 and TGF- β and contribute to fibrosis progression. miR-146b-5p is a potential biomarker and therapeutic target for HF.

Introduction

Hepatic fibrosis (HF) is a pathological change caused by various reasons during the repair process of chronic liver injuries. It is a pre-pathological change of liver cirrhosis and may even progress to liver cancer (1). Hepatic stellate cells (HSCs) are the main effector cells involved in HF (2). Excessive production of the extracellular matrix (ECM) secreted by HSCs in the liver is the key event in the development of HF (3,4). Following activation of HSCs, the deposition of ECM causes damage to liver tissues. Eventually, abnormally activated signaling pathways result in malignant cell growth, migration and gene expressions; thus finally leading to HF (5). So far, clinical management of HF has been a global challenge that lacks effective treatment and there is an urgent need to explore the options for treatment.

MicroRNAs (miRNAs/miRs) are short non-coding RNAs comprising only 20-24 amino acids. They are vital epigenetic regulators in post-transcriptional translation and they are closely linked to the development of human diseases (6). miR-122 and miR-16 are very important during the development of HF through mediating the proliferation, activation and apoptosis of HSCs (7,8).

Homeodomain interacting protein kinase 1 (HIPK1) is a serine/threonine kinase located in the nucleus. It serves an important role in regulating cell proliferation, activation and apoptosis through mediating oligomerization of apoptosis signal-regulating kinase 1 and activation of the mitogen-activated protein kinase signaling pathway (9-11). HIPK1 also participates in the DNA damage repair (12). However, the role of HIPK1 in HF has not yet been reported. Our previous studies have shown that overexpression of HIPK1 in the rat HSC cell line HSC-T6 can downregulate downstream transforming growth factor β (TGF- β), α -smooth muscle actin (α -SMA) and collagen type I α 1 chain (COL1A1), which are

Correspondence to: Professor Tianxin Xiang, Department of Hospital Infection Control, The First Affiliated Hospital of Nanchang University, 17 Yongwaizheng Street, Donghu, Nanchang, Jiangxi 330000, P.R. China
E-mail: txxiangmed@163.com

*Contributed equally

Key words: hepatic fibrosis, miR-146b-5p, homeodomain interacting protein kinase 1, hepatic stellate cells

closely associated with HF, suggesting that HIPK1 may be a target for inhibiting HSC activation.

To explore the possible regulatory mechanism in the process of HF, the present study constructed a rat model of HF and found the abnormal expression of miR-146b-5p and HIPK1. The present study hypothesized that HSC activation could upregulate miR-146b-5p, thus contribute to the progression of HF.

Materials and methods

Establishment of the rat HF model. A total of 12 male Sprague-Dawley (SD) rats aged 6 weeks, weighing 180-220 g were provided by the Guangdong Medical Laboratory Animal Center. The rats were habituated in a specific pathogen-free environment at $22\pm 2^{\circ}\text{C}$, with a 12/12-h light/dark cycle and free access to food and water. Rats were randomly divided into the control group ($n=6$) and HF group ($n=6$). Rats in the HF group were subcutaneously injected with 0.3 ml/100 g carbon tetrachloride (CCl_4) three times a week, for eight consecutive weeks, while rats in the control group were subcutaneously injected with the same volume of normal saline. All rats were sacrificed at the end of the eighth week and the tissues which were 1.5 cm from the lower edge of the left lobe of the liver were collected for subsequent experiments. When the rats quickly lost more than 20% of their original body weight, could not eat or drink, exhibited mental depression with hypothermia, suffered body organ infection or severe liver failure, the experiment was stopped and the rats sacrificed. The rats were sacrificed by intraperitoneal injection of sodium pentobarbital with an injection dose of 200 mg/kg. According to AVMA Guidelines for the Euthanasia of Animals: 2020 Edition (<https://www.avma.org/resources/pet-owners/petcare/euthanasia>), mortality was confirmed by checking that the hearts had stopped beating for 2 min and the respiratory arrest was also observed. The animal research of this project was approved by the medical research ethics committee of the First Affiliated Hospital of Nanchang University, ethics approval no. 2020117.

Hematoxylin and eosin (H&E) staining. Rat liver tissues were fixed in 4% paraformaldehyde for 24 h at room temperature, dehydrated and transparentized with gradient concentrations (30, 50, 75, 95 and 100%) of ethanol and xylene, and then embedded in paraffin at 55°C to prepare 4- μm tissue sections. Next, they were immersed twice in xylene for 20 min, twice in anhydrous ethanol for 5 min and in 75% ethanol for 5 min and finally washed in ddH_2O . The H&E staining kit (Sangon Biotech Co., Ltd.; cat. no. E607318) was used in the present study. Briefly, sections were stained with hematoxylin for 5 min at room temperature. Following differentiation and bluing, they were washed in ddH_2O , dehydrated in 85% and 5% ethanol sequentially and stained with eosin for 5 min at room temperature. After incubating three times in anhydrous ethanol and twice in xylene, they were mounted using neutral gum for observation under a light microscope. A total of five fields of view were randomly selected for each tissue section and observed at x100 magnification.

Masson staining. Rat liver tissues were dewaxed and dehydrated in xylene and ethanol with gradient concentrations

(100, 85, 75 and 30%). After nuclei staining using the Weigert's iron hematoxylin solution for 5-10 min and washing in flowing water, sections were later counterstained with Ponceau S and acid fuchsin for 5-10 min. Following washing in 2% acetic acid aqueous solution, differentiation in 1% phosphomolybdic acid solution for 3-5 min, staining in aniline blue WS for 5 min and washing in 0.2% acetic acid aqueous solution, sections were washed in 95% ethanol and anhydrous ethanol. All the aforementioned steps were performed at room temperature. Sections were permeabilized using xylene, mounted using neutral gum and observed under a light microscope. A total of five fields of view were randomly selected for each tissue section and observed at x100 magnification.

Immunohistochemistry (IHC). Rat liver sections were incubated three times in xylene for 15 min and they were dehydrated twice in anhydrous ethanol for 5 min, 85% ethanol for 5 min and 75% ethanol for 5 min. After washing in ddH_2O , sections were immersed in citrate buffer (pH 6.0, Sangon Biotech Co., Ltd.; cat. no. E673000) for 15 min antigen retrieval at room temperature. They were incubated in 3% H_2O_2 in the dark for 25 min and blocked in 3% BSA (Sangon Biotech Co., Ltd.; cat. no. E661003) at 37°C for 30 min. Incubation of primary antibodies was performed at 4°C overnight, and on the next day, sections were washed three times in PBS (pH 7.4) for 5 min and incubated with HRP-labeled secondary antibodies (ABclonal Biotech Co., Ltd.; cat. no. AS029; 1:500 dilution) at room temperature for 2 h. Later, sections were counterstained with DAB and hematoxylin for 3 min to distinguish between cytoplasm and nucleus. After dehydration in ddH_2O , 75% ethanol for 5 min, 85% ethanol for 5 min, twice in anhydrous ethanol for 5 min and n-butanol for 5 min and permeabilization in xylene for 5 min, sections were mounted using neutral gum. Positive staining of cells was observed under a microscope (XSP-8CA; Shanghai Optical Instrument Co. Ltd.). A total of five fields of view were randomly selected for each tissue section and observed at x100 magnification. The following primary antibodies (1:200 dilution) were purchased from ABclonal Biotech Co., Ltd.: α -SMA (cat. no. A17910) and HIPK1 (cat. no. A7414).

Cell culture. The rat HSC cell line HSC-T6 (Procell Life Science & Technology Co., Ltd.; cat. no. CL-0116) was cultivated in Dulbecco's Modified Eagle Medium (DMEM) (Procell Life Science & Technology Co., Ltd.; cat. no. 164210-500) containing 10% FBS (Procell Life Science & Technology Co., Ltd.; cat. no. PM150210) and 1% penicillin and streptomycin in a humidified incubator containing 5% CO_2 and 95% air at 37°C . Cryopreservation using DMEM containing 40% FBS, 10% DMSO and 55% glucose was performed until the cells reached a confluence of more than 80% by trypsin digestion.

293T cells were purchased from the ATCC and used for lentiviral packaging. The cell culture protocol was the same as that of HSC-T6 cells. When the cells were >80% confluent, they were digested with trypsin and inoculated into a new culture dish. When the cells were adherent, they were incubated with serum-free Opti-MEM (Gibco; Thermo Fisher Scientific, Inc.) for 4 h, after which transfection and lentiviral packaging were performed.

HSC-T6 cell activation. HSC-T6 cell activation was performed by lipopolysaccharide (LPS) induction at 37°C for 48 h. Briefly, cells were cultured in DMEM containing 10% FBS, 1% penicillin and streptomycin and 0.1 µg/ml LPS at 37°C. At 48 h, the expression level of the HF marker α -SMA in HSC-T6 cells was determined using RT-qPCR and western blotting. Upregulated α -SMA suggested activation of HSC-T6 cells.

Cell transfection. miR-146b-5p mimics, miR-146b-5p inhibitor and their negative controls mimic-NC and inhibitor-NC were provided by RiboBio Co., Ltd. (Guangzhou, China) (mimics: 5'-UGAGAACUGAAUCCAUAAGGCUGU-3'; mimic-NC: 5'-UUCUCCGAACGUGUCACGUTT-3'; inhibitor: 5'-ACA GCCUAUGGAAUUCAGUUCUCA-3'; inhibitor-NC: 5'-CAG UACUUUUGUGUAGUACAA-3'). Lipofectamine® 2000 reagent (Invitrogen; Thermo Fisher Scientific, Inc.) was used for cell transfection. Briefly, cells were seeded in a 12-well plate (1x10⁵ cells per well) and cultured to 80% confluence. After 4-h starvation in serum-free DMEM, a 100 nM transfection mixture containing the mimics, inhibitor or the mimic-NC or inhibitor-NC (1.6 µg/well) and Lipofectamine® 2000 reagent (4 µl/well) was added for 40 min incubation at 37°C. Fresh medium was replaced at 24 h and transfection efficacy was examined by reverse transcription-quantitative (RT-q)PCR. Subsequent experiments were performed 2 weeks after the transfection experiment.

RT-qPCR. Total RNAs in HSC-T6 cells or liver tissues were isolated using TRIzol® (Thermo Fisher Scientific, Inc.), and 1 µg total RNA was reverse transcribed to cDNA using the Takara PrimeScript RT reagent kit. Subsequently, qPCR was performed using a SYBR Premix Ex Taq II with Tli RNaseH (Takara Bio, Inc.) on an ABI Prism 7500 system (Thermo Fisher Scientific, Inc.). All experimental steps were performed in accordance with the manufacturer's protocols. In brief, total RNA induced with gDNA eraser and reverse transcribed to cDNA was subjected to thermocycling at 95°C for 15 min, followed by 40 cycles at 95°C for 5 sec, 60°C for 30 sec and 72°C for 40 sec and finally annealing at 72°C for 10 min. The relative level was measured using an ABI Prism 7500 system (Thermo Fisher Scientific, Inc.) and calculated using the 2^{- $\Delta\Delta C_q$} method with GAPDH or U6 as the internal reference (13). Each experiment was repeated three times. Primer sequences are listed in Table I.

Western blotting. Total proteins in HSC-T6 cells or liver tissues were isolated using RIPA buffer (Beyotime Institute of Biotechnology) containing phenylmethylsulfonyl fluoride and protease inhibitor. Protein concentrations were measured using the BCA protein assay kit (Beyotime Institute of Biotechnology). Protein samples (50 µg) were loaded onto 10% gels for sodium dodecyl sulfate-polyacrylamide gel electrophoresis (SDS-PAGE) and transferred on polyvinylidene fluoride (PVDF) membranes at 300 mA. Non-specific antigens on PVDF membranes were blocked by immersing in 1X TBST (0.1% Tween) containing 5% skimmed milk. After immunoblotting with primary antibodies (1:1,000) at 4°C overnight and secondary antibodies (1:1,000) at room temperature for 1 h, band exposure was performed using the Bio-Rad Universal Hood II Gel Doc Imaging system and the gray value

Table I. Primers used in the present study.

Gene	Primers (5'-3')
Rno-miR-146b-5p-F	AACACGCTGAGAACTGAATTCC
Rno-miR-146b-5p-R	GTCGTATCCAGTGCAGGGTCCG AGGTATTTCGCACTGGATACGAC ACAGCC
HIPK1-F	CAGCATCAGCCAATCATC
HIPK1-R	ATTAGACCTCGCCTTCAG
α -SMA-F	CCGAGATCTCACCGACTACC
α -SMA-R	TCCAGAGCTACATAGCACAG
COL1A1-F	CCGAGGTATGCTTGATCT
COL1A1-R	GACAGTCCAGTTCTTCATTG
TGF- β -F	CACCATCCATGACATGAACC
TGF- β -R	TCATGTTGGACAACCTGCTCC
GAPDH-F	AAGCTCACTGGCATGGCCTT
GAPDH-R	CGGCATGTCAGATCCACAAC
U6-F	CTCGCTTCGGCAGCAC
U6-R	AACGCTTCACGAATTTGCGT

miR, microRNA; HIPK1, homeodomain interacting protein kinase 1; F, forward; R, reverse; α -SMA, α -smooth muscle actin; COL1A1, collagen type I α 1 chain; TGF- β , transforming growth factor β .

was analyzed using ImageJ v. 1.8.0.112 (National Institutes of Health). All the antibodies were purchased from Abclonal as listed: α -SMA (cat. no. A17910), COL1A1 (cat. no. A1352), TGF- β (cat. no. A18692), HIPK1 (cat. no. A19580), GAPDH (cat. no. A19056) and the secondary antibody (cat. no. AS014).

MTT assay. HSC-T6 cells were seeded in a 96-well plate (5x10³ cells per well) and 200 µl of DMEM containing 10% FBS and 1% penicillin and streptomycin was added per well. Briefly, 15 µl of MTT solution (15 mg/ml, Sangon Biotech Co., Ltd.; cat. no. A600799) was added at the indicated time points at 37°C. After cell culture for 4 h, cells per well were lysed in 150 µl of DMSO for 10 min at room temperature and optical density at 490 nm was measured using the HBS-1101 microplate reader (Nanjing Detie Experimental Equipment Co., Ltd.).

Dual-luciferase reporter assay. The wild-type plasmid pGL3-HIPK1-WT was constructed by amplifying complementary sequences in the HIPK1 3'UTR and the promoter region of miR-146b-5p and cloning them into the pGL3 3'UTR (Shanghai GeneChem Co., Ltd.). The mutant-type plasmid pGL3-HIPK1-Mut was constructed using the site-directed mutagenesis kit (Sangon Biotech Co., Ltd.; cat. no. B639281). Wild-type and mutant-type plasmids were co-transfected into cells with miR-146b-5p mimics or mimics-NC and Lipofectamine 2000 (Invitrogen; Thermo Fisher Scientific, Inc.) for 48 h. Relative Firefly and Renilla luciferase activities were measured using the Dual-Luciferase Reporter Gene Assay kit (Promega Corporation).

Lentivirus infection. Overexpressing lentivirus plasmid GV367-HIPK1 (Shanghai GeneChem Co., Ltd.) was generated

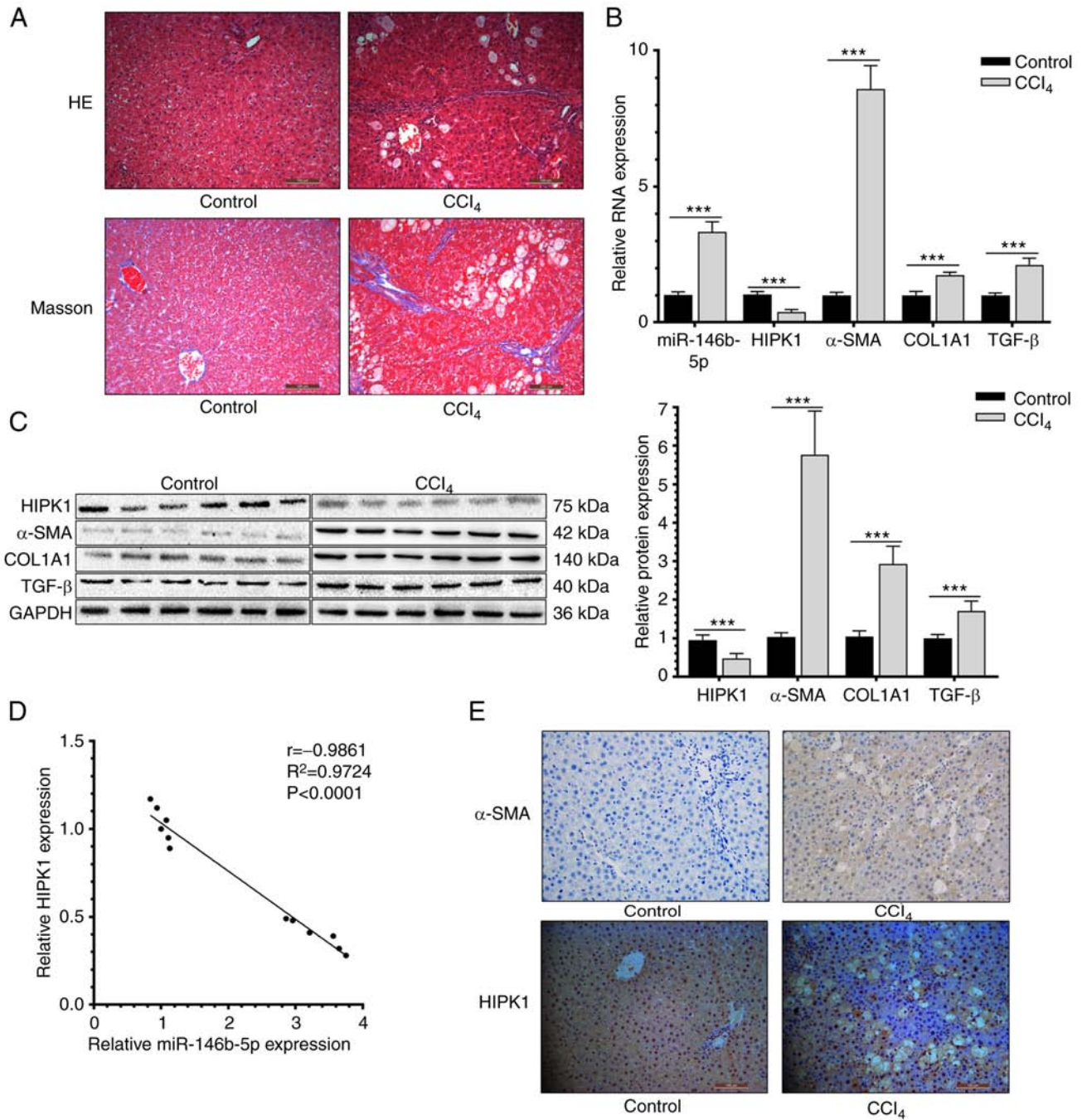


Figure 1. miR-146b-5p is upregulated and HIPK1 is downregulated in rats with HF. (A) HE staining and Masson staining of normal and HF rats hepatic tissues (x200 magnification). (B) Relative miR-146b-5p, HIPK1, α -SMA, COL1A1 and TGF- β RNA expression of normal and HF rats hepatic tissues. (C) Relative HIPK1, α -SMA, COL1A1 and TGF- β protein expression of normal and HF rats hepatic tissues. (D) Correlation between HIPK1 and miR-146b-3p expression. (E) α -SMA and HIPK1 expression in normal and HF rats hepatic tissues (x200 magnification). ***P<0.001. miR, microRNA; HIPK1, homeodomain interacting protein kinase 1; HF, hepatic fibrosis; HE, hematoxylin and eosin; α -SMA, α -smooth muscle actin; COL1A1, collagen type I α 1 chain; TGF- β , transforming growth factor β .

by cleavage of the GV367 plasmid using *AgeI/NheI* and GV367 was used as blank control. Lentivirus packaging was performed using the second-generation lentivirus packaging kit (Shanghai GeneChem Co., Ltd.). The lentiviral plasmid, packaging vector and envelope vector were mixed at a 4:3:2 ratio for a total DNA mass of 20 μ g and incubated with 1 ml of Lenti-Easy Packaging Mix (Shanghai GeneChem Co., Ltd.) for 15 min. The mixture was then incubated for another 20 min in Lipofectamine 2000 (Invitrogen; Thermo Fisher Scientific, Inc.) and it was applied into 293T cell culture

medium for 6 h at 37°C. 293T cells were seeded in a 12-well plate at a density of 2.5×10^5 cells/well and cultured to 80% confluence. After incubation in serum-free DMEM for 4 h, cells were transfected as mentioned above with lentiviruses for 3 days. Transfected cells were filtered using a 0.45 μ m mesh, which were concentrated at 70,000 g at 4°C for 2 h. The supernatant was collected for detecting viral titers. HSC-T6 cells cultured to more than 80% confluence were cultured with diluted lentiviruses and GFP-labeled cells with lentivirus transfection rate >80% at 72 h were screened

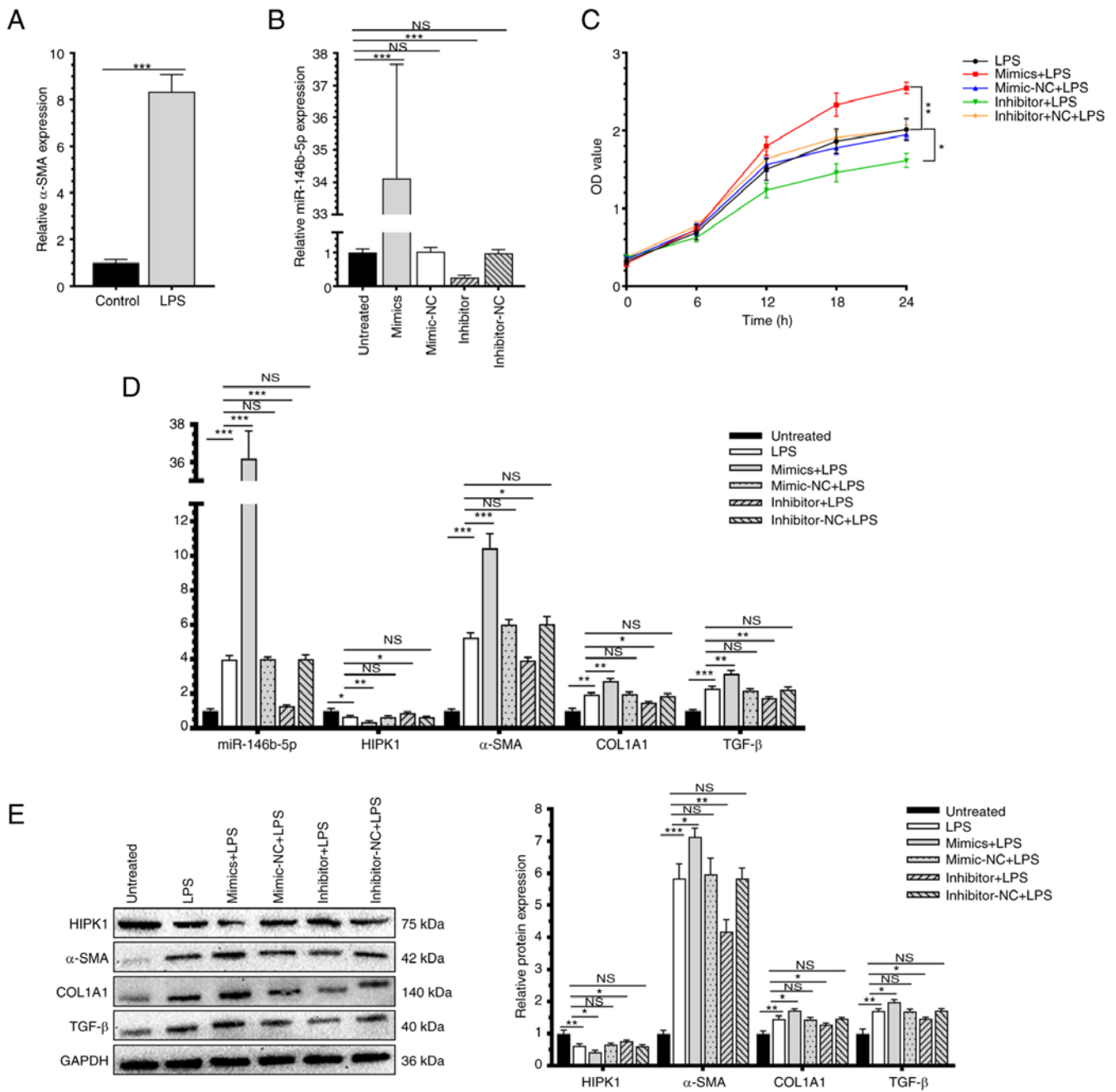


Figure 2. miR-146b-5p upregulates the fibrosis markers in HSCs. (A) α -SMA is upregulated *in vitro* cell model with LPS treatment. (B) miR-146b-5p transfection efficiency. (C) Cell viability of HSC-T6 transfected with miR-146b-5p mimics, inhibitor or NCs and treated with LPS (compared with untreated group). (D) Relative miR-146b-5p, HIPK1, α -SMA, COL1A1 and TGF- β RNA expression. (E) Relative HIPK1, α -SMA, COL1A1 and TGF- β protein expression. * P <0.05; ** P <0.01; *** P <0.001. miR, microRNA; HSCs, hepatic stellate cells; α -SMA, α -smooth muscle actin; LPS, lipopolysaccharide; NCs, negative controls; HIPK1, homeodomain interacting protein kinase 1; COL1A1, collagen type I α 1 chain; TGF- β , transforming growth factor β ; NS, no significance.

out. Transfection efficacy of HIPK1 was finally verified by RT-qPCR.

Statistical analysis. Data were expressed as mean \pm standard deviation from three replicates and processed by GraphPad Prism 8.0 (GraphPad Software, Inc.). Differences between groups were compared by the unpaired Student's *t* test. One-way ANOVA was used to assess differences among the groups and Tukey's and Bonferroni's tests were used for post hoc testing following ANOVA. Pearson's analysis was used in correlation analysis between miR-146b-5p and HIPK1. P <0.05 was considered to indicate a statistically significant difference.

Results

miR-146b-5p is upregulated in rats with HF. An *in vivo* HF model in rats was established by administering a subcutaneous injection of CCl_4 for 8 weeks. After sacrifice, rat liver tissues were collected and prepared for H&E staining, Masson staining, IHC, RT-qPCR and western blotting. Compared with rat liver tissues from the control group, tissues from the HF group presented mixed nodules of varying sizes and a widened fibrosis interval (Fig. 1A). In addition, upregulated mRNA levels of miR-146b-5p, α -SMA, COL1A1 and TGF- β , as well as upregulated protein

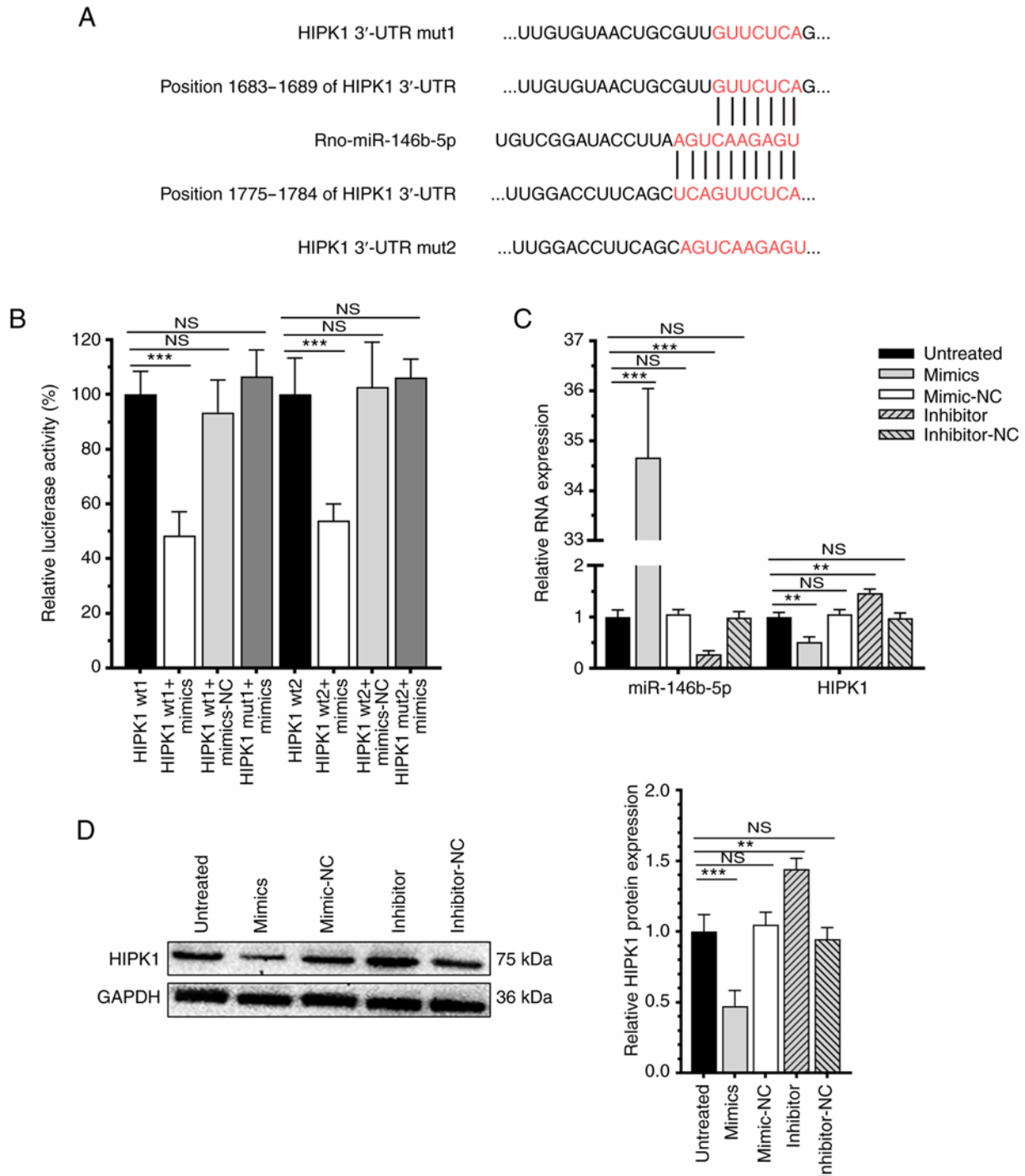


Figure 3. miR-146b-5p directly targets HIPK1 and downregulates its expression level. (A) Prediction of the targeting relationship between HIPK1 and rno-miR-146b-5p. (B) Dual-luciferase reporter assay. (C) Relative HIPK1 mRNA expression transfected with miR-146b-5p mimics. (D) Relative HIPK1 protein mRNA expression transfected with miR-146b-5p mimics. ** $P < 0.01$; *** $P < 0.001$. miR, microRNA; HIPK1, homeodomain interacting protein kinase 1; NS, no significance; NC, negative control.

levels of α -SMA, COL1A1 and TGF- β , were observed in HF liver tissues (Fig. 1B and C). A negative correlation was identified between the relative levels of miR-146b-5p and HIPK1 (Fig. 1D). As shown in IHC staining images, the HIPK1 was significantly observed both in cytoplasmic and nuclear regions and the expression level of HIPK1 was significantly downregulated in liver sections from the HF group, while the level of α -SMA was upregulated compared with those in the control group (Fig. 1E). This suggested

that upregulated miR-146b-5p in liver tissues of rats with HF could be involved in the progression of HF.

miR-146b-5p upregulates the fibrosis markers in HSCs. HSC-T6 cells were induced with 0.1 μ g/ml LPS treatment and then the upregulated mRNA level of α -SMA validated the activation of HSCs (Fig. 2A). The present study first examined the transfection efficacy of miR-146b-5p mimics and inhibitor in HSC-T6 cells by RT-qPCR (Fig. 2B). As revealed by the

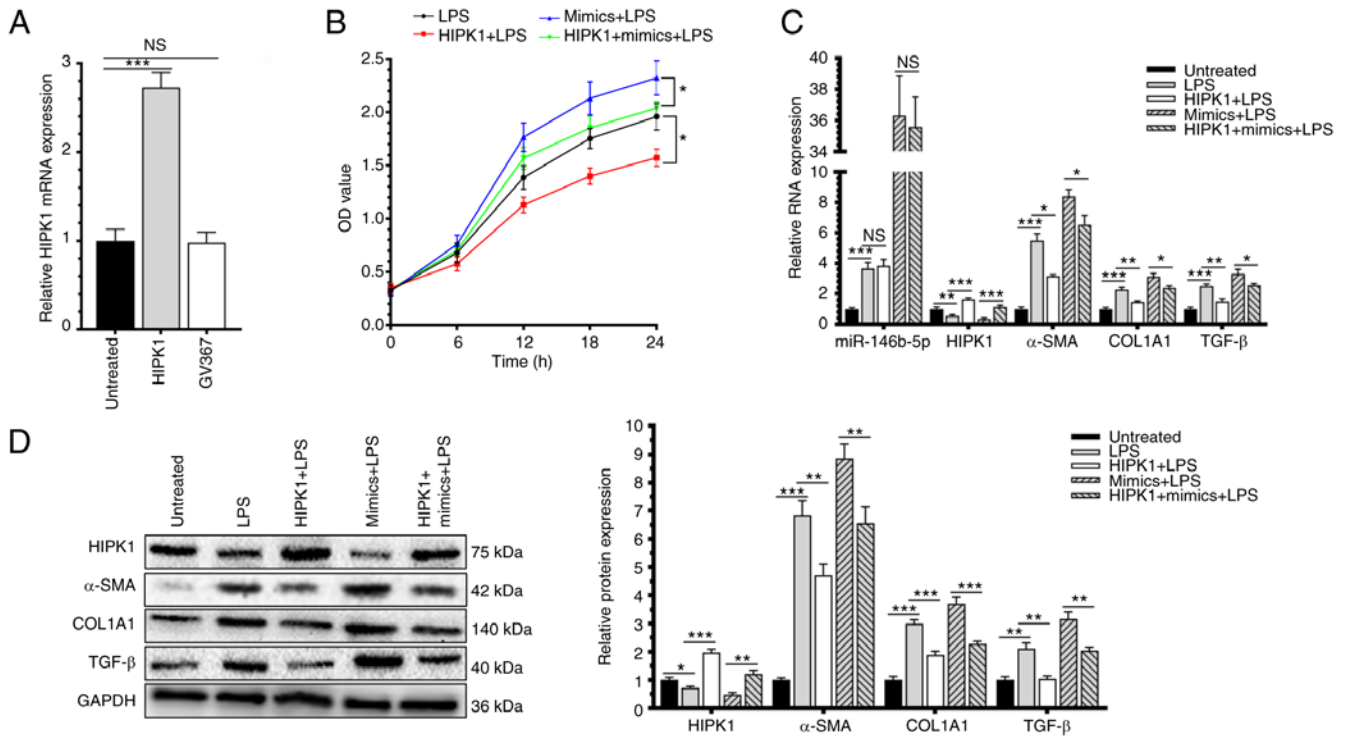


Figure 4. Overexpression of HIPK1 effectively decreases the effect of miR-146b-5p in contribution to the progression of HF. (A) Transfection efficiency of lentivirus. (B) Cell viability of HSC-T6. (C) Relative miR-146b-5p, HIPK1, α -SMA, COL1A1 and TGF- β RNA expression. (D) Relative HIPK1, α -SMA, COL1A1 and TGF- β protein expression. * $P < 0.05$; ** $P < 0.01$; *** $P < 0.001$. HIPK1, homeodomain interacting protein kinase 1; NS, no significance; miR, microRNA.

MTT assay, overexpression of miR-146b-5p enhanced the viability of LPS-induced HSC-T6 cells and knockdown of miR-146b-5p reduced the cell viability (Fig. 2C). In addition, transfection of miR-146b-5p mimics upregulated the mRNA and protein levels of HF markers α -SMA, COL1A1 and TGF- β and downregulated the level of HIPK1. Knockdown of miR-146b-5p led to an opposite trend (Fig. 2D and E). It can be concluded that miR-146b-5p stimulated the activation of HSCs and upregulated the fibrosis markers in HSCs.

miR-146b-5p directly targets HIPK1 and downregulates its expression level. Using TargetScan 7.2 and StarBase 3.0, miR-146b-5p was predicted to bind to the HIPK1 and HIPK2 3'UTR (Figs. 3A and S1). Subsequently, the dual-luciferase reporter assay showed that overexpression of miR-146b-5p specifically reduced the luciferase activity of pGL3-HIPK1-WT, but the luciferase activity of pGL3-HIPK1-MuT was not affected (Fig. 3B), confirming the binding between miR-146b-5p and HIPK1. Moreover, transfection of miR-146b-5p mimics significantly downregulated the mRNA and protein levels of HIPK1 and transfection of the miR-146b-5p inhibitor upregulated the mRNA and protein levels of HIPK1 (Fig. 3C and D). Collectively, miR-146b-5p could target the HIPK1 3'UTR and downregulate HIPK1 through inhibiting the transcription.

Overexpression of HIPK1 effectively decreased the effect of miR-146b-5p in HSC-T6 activation. To further explore the role of HIPK1 in the progression of HF, its level was intervened by lentivirus transfection (Fig. 4A). After co-intervention of HIPK1 and miR-146b-5p in HSC-T6 cells, they were activated

by LPS induction. Overexpression of HIPK1 significantly reduced the viability of LPS-induced HSC-T6 cells and interestingly, it could effectively decrease the positive effect of overexpressed miR-146b-5p in promoting the cell viability (Fig. 4B). In addition, the upregulated mRNA and protein levels of α -SMA, COL1A1 and TGF- β in LPS-induced HSC-T6 cells overexpressing miR-146b-5p were markedly decreased by the overexpression of HIPK1 (Fig. 4C and D). Therefore, HIPK1 was responsible for the regulatory effect of miR-146b-5p in the activation of HSC-T6, thus may contribute to fibrosis progression.

Discussion

HF is the most common type of chronic liver disease and it is a scar formation process following liver injury (14). It is characterized by excessive deposition of ECM resulting from the activation of HSCs (15). A damaged liver structure, formation of nodules, scar repair and activation of multiple signaling pathways eventually lead to irreversible liver cirrhosis and even liver cancer (4). So far, liver transplantation and drug treatment are available in severe liver diseases, although their clinical applications are markedly limited by high medical costs and low survival rate (16). Therefore, it is important to search for potential targets that can regulate HSC activation, which is conducive to the clinical management of HF.

Biological functions of miRNAs in tumors (17), atherosclerosis (18), metabolic syndrome (19) and other diseases have gradually emerged. With increased clinical research on miRNAs, their vital involvement in liver diseases has been recognized. Accumulating evidence has shown that miRNAs

are able to regulate the activation and proliferation of HSCs and thus they mediate the progression of HF. Riaz *et al* (20) reported that miR-188-5p alleviates the severity of HF through inhibiting the activation and proliferation of HSCs via the PTEN/AKT pathway. Li *et al* (21) proved that miR-34c promotes HSC activation and the progression of HF by targeting the key enzyme ACSL1 that affects fatty acid synthesis. Overexpression of miR-494-3p suppresses HSC activation through inhibiting proliferation and inducing apoptosis by targeting TRAF3 (22). miR-146b has been extensively analyzed in pancreatic cancer (23), colorectal cancer (24), thyroid cancer (25) and gallbladder cancer (26), while its biological function in the progression of HF has been rarely reported. Ge *et al* (27,28) revealed that miR-146b promotes the activation and proliferation of HSCs and the HMGB1/p65/miR-146b/HNF1A axis exerts a key effect on regulating HSC functions and HF. In the present study, miR-146b-5p was significantly upregulated in liver tissues of rats with HF than in liver tissues of normal rats. In addition, both the mRNA and protein levels of HF markers α -SMA, COL1A1 and TGF- β were upregulated. Overexpression of miR-146b-5p markedly enhanced LPS-induced activated HSC-T6 cells and correspondingly, the mRNA and protein levels of HF markers α -SMA, COL1A1 and TGF- β were upregulated. As expected, transfection of the miR-146b-5p inhibitor resulted in an opposite trend. Consistent with previous findings, the results of the present study showed that miR-146b-5p was able to induce the activation of HSCs and upregulate HF markers; thus suggesting that miR-146b-5p may serve an important role during the progression of HF.

HIPK1 is a regulator of transcription factors containing the homology domains (29). The tumor suppressor role of HIPK1 has been revealed in numerous types of tumors due to its regulatory effects on cell apoptosis and DNA damage repair (30). Palkina *et al* (31) validated that miR-3065-5p inhibits proliferation and alters cell cycle distribution of melanoma cells by targeting HIPK1. Rey *et al* (10) proposed that HIPK1 is significantly upregulated in colorectal cancer (CRC) in a stage-dependent manner, which restricts the uncontrolled growth of CRC cells by activating the p53 signaling pathway. A number of efforts have been made to explore the role of HIPK1 in tumors, kidney diseases and diabetes (32). Its function in HF has not yet been reported. The present study showed that compared with rats in the control group, the mRNA and protein levels of HIPK1 in rat liver tissues from the HF group were significantly downregulated. In addition, the miR-146b-5p level was negatively correlated with the level of HIPK1 in rats liver and as predicted by using TargetScan 7.2 and StarBase 3.0, miR-146b-5p was able to target the HIPK1 3'UTR and regulate its expression, indicating a potential binding relationship between them. Subsequently, it was confirmed by the dual-luciferase reporter assay that miR-146b-5p could directly target with HIPK1. Transfected with miR-146b-5p significantly downregulated the expression of HIPK1. Notably, overexpression of HIPK1 by lentivirus transfection markedly decreased the effects of miR-146b-5p in enhancing the viability and upregulating the HF markers α -SMA, COL1A1 and TGF- β in LPS-induced activated HSC-T6 cells. In addition, it is worth noting that the present study was based on the rats HF model and combined this with cell experiments to research the molecular mechanism. Although it has a

certain correlation with human HF, the present study did not involve any samples of clinical patients; and according to the TargetScan 7.2 prediction, miR-146b-5p could also directly target with HIPK2; however, this potential association was not investigated in the present study; moreover, since the miR-146b-5p is a miRNA, which does not encode any protein, the histology of liver sections in hepatic fibrosis cannot show the interaction of miR-146b-5p and HIPK1. The present study also did not verify the reversal effect of miR-146b-5p on HF in rat model, which is one of its the limitations. Therefore, further in-depth research is needed to explore its clinical application. Taken together, miR-146b-5p promoted the activation of HSCs and contributed to the progression of HF by targeting and downregulating HIPK1.

miR-146b-5p was significantly upregulated during the progression of HF. Overexpressed miR-146b-5p could significantly activate HSCs, upregulate α -SMA, COL1A1 and TGF- β and thus contribute to the progression of HF via directly targeting and downregulating HIPK1. miR-146b-5p is a potential biomarker and therapeutic target for HF.

Acknowledgements

Not applicable.

Funding

The present study was funded by Jiangxi Outstanding Talents Fund (grant no. 20192BcB23022), National Natural Science Foundation Youth Project (grant no. 81900561) and National Natural Science Foundation Regional Project (grant nos. 81760115 and 81960121).

Availability of data and materials

The datasets used and/or analyzed during the current study are available from the corresponding author on reasonable request.

Authors' contributions

JX, NC and TX made substantial contributions to conception, design and acquisition of data. ZH and XS made substantial contributions to the analysis and interpretation of the data. All authors contributed to the writing of the article and have read and approved the manuscript. JX and TX confirm the authenticity of all the raw data.

Ethics approval and consent to participate

The animal research of the present study was approved by the Medical Research Ethics Committee of the First Affiliated Hospital of Nanchang University (ethics approval no. 2020117).

Patient consent for publication

Not applicable.

Competing interests

The authors declare that they have no competing interests.

References

- Hernandez-Gea V and Friedman SL: Pathogenesis of liver fibrosis. *Annu Rev Pathol* 6: 425-456, 2011.
- Hou W and Syn WK: Role of metabolism in hepatic stellate cell activation and fibrogenesis. *Front Cell Dev Biol* 6: 150, 2018.
- Lee UE and Friedman SL: Mechanisms of hepatic fibrogenesis. *Best Pract Res Clin Gastroenterol* 25: 195-206, 2011.
- Jung YK and Yim HJ: Reversal of liver cirrhosis: Current evidence and expectations. *Korean J Intern Med* 32: 213-228, 2017.
- Mekala S, Tulimilli SV, Geesala R, Manupati K, Dhoke NR and Das A: Cellular crosstalk mediated by platelet-derived growth factor BB and transforming growth factor beta during hepatic injury activates hepatic stellate cells. *Can J Physiol Pharmacol* 96: 728-741, 2018.
- Bartel DP: MicroRNAs: Genomics, biogenesis, mechanism, and function. *Cell* 116: 281-297, 2004.
- Nakamura M, Kanda T, Sasaki R, Haga Y, Jiang X, Wu S, Nakamoto S and Yokosuka O: MicroRNA-122 inhibits the production of inflammatory cytokines by targeting the PKR activator PACT in human hepatic stellate cells. *PLoS One* 10: e0144295, 2015.
- Yu F, Chen B, Fan X, Li G, Dong P and Zheng J: Epigenetically-regulated MicroRNA-9-5p suppresses the activation of hepatic stellate cells via TGFBR1 and TGFBR2. *Cell Physiol Biochem* 43: 2242-2252, 2017.
- Li X, Luo Y, Yu L, Lin Y, Luo D, Zhang H, He Y, Kim YO, Kim Y, Tang S and Min W: SENP1 mediates TNF-induced desumoylation and cytoplasmic translocation of HIPK1 to enhance ASK1-dependent apoptosis. *Cell Death Differ* 15: 739-750, 2008.
- Rey C, Soubeyran I, Mahouche I, Pedeboscq S, Bessede A, Ichas F, De Giorgi F and Lartigue L: HIPK1 drives p53 activation to limit colorectal cancer cell growth. *Cell Cycle* 12: 1879-1891, 2013.
- van der Laden J, Soppa U and Becker W: Effect of tyrosine autophosphorylation on catalytic activity and subcellular localisation of homeodomain-interacting protein kinases (HIPK). *Cell Commun Signal* 13: 3, 2015.
- Kondo S, Lu Y, Debbas M, Lin AW, Sarosi I, Itie A, Wakeham A, Tuan J, Saris C, Elliott G, *et al*: Characterization of cells and gene-targeted mice deficient for the p53-binding kinase homeodomain-interacting protein kinase 1 (HIPK1). *Proc Natl Acad Sci USA* 100: 5431-5436, 2003.
- Livak KJ and Schmittgen TD: Analysis of relative gene expression data using real-time quantitative PCR and the 2(-Delta Delta C(T)) method. *Methods* 25: 402-408, 2001.
- Kisseleva T and Brenner DA: Mechanisms of fibrogenesis. *Exp Biol Med (Maywood)* 233: 109-122, 2008.
- Iwaisako K, Jiang C, Zhang M, Cong M, Moore-Morris TJ, Park TJ, Liu X, Xu J, Wang P, Paik YH, *et al*: Origin of myofibroblasts in the fibrotic liver in mice. *Proc Natl Acad Sci USA* 111: E3297-E3305, 2014.
- Jesudian A, Desale S, Julia J, Landry E, Maxwell C, Kallakury B, Laurin J and Shetty K: Donor factors including donor risk index predict fibrosis progression, allograft loss, and patient survival following liver transplantation for hepatitis C virus. *J Clin Exp Hepatol* 6: 109-114, 2016.
- Winkle M, El-Daly SM, Fabbri M and Calin GA: Noncoding RNA therapeutics-challenges and potential solutions. *Nat Rev Drug Discov* 20: 629-651, 2021.
- Ali Sheikh MS, Alduraywish A, Almaeen A, Alruwali M, Alruwaili R, Alomair BM, Salma U, Hedeab GM, Bugti N and Abdulhabeeb IAM: Therapeutic value of miRNAs in coronary artery disease. *Oxid Med Cell Longev* 2021: 8853748, 2021.
- Fodor A, Lazar AL, Buchman C, Tiperciuc B, Orasan OH and Cozma A: MicroRNAs: The link between the metabolic syndrome and oncogenesis. *Int J Mol Sci* 22: 6337, 2021.
- Riaz F, Chen Q, Lu K, Osoro EK, Wu L, Feng L, Zhao R, Yang L, Zhou Y, He Y, *et al*: Inhibition of miR-188-5p alleviates hepatic fibrosis by significantly reducing the activation and proliferation of HSCs through PTEN/PI3K/AKT pathway. *J Cell Mol Med* 25: 4073-4087, 2021.
- Li B, Liu J, Xin X, Zhang L, Zhou J, Xia C, Zhu W and Yu H: MiR-34c promotes hepatic stellate cell activation and liver fibrogenesis by suppressing ACSL1 expression. *Int J Med Sci* 18: 615-625, 2021.
- Li H, Zhang L, Cai N, Zhang B and Sun S: MicroRNA-494-3p prevents liver fibrosis and attenuates hepatic stellate cell activation by inhibiting proliferation and inducing apoptosis through targeting TRAF3. *Ann Hepatol* 23: 100305, 2021.
- Zhou M, Gao Y, Wang M, Guo X, Li X, Zhu F, Xu S and Qin R: MiR-146b-3p regulates proliferation of pancreatic cancer cells with stem cell-like properties by targeting MAP3K10. *J Cancer* 12: 3726-3740, 2021.
- Wang D, Feng M, Ma X, Tao K and Wang G: Transcription factor SP1-induced microRNA-146b-3p facilitates the progression and metastasis of colorectal cancer via regulating FAM107A. *Life Sci* 277: 119398, 2021.
- Liu X, Fu Q, Bian X, Fu Y, Xin J, Liang N, Li S, Zhao Y, Fang L, Li C, *et al*: Long non-coding RNA MAPK8IP2 inhibits lymphatic metastasis of thyroid cancer by activating hippo signaling via sponging miR-146b-3p. *Front Oncol* 10: 600927, 2021.
- Ouyang B, Pan N, Zhang H, Xing C and Ji W: miR146b5p inhibits tumorigenesis and metastasis of gallbladder cancer by targeting Tolllike receptor 4 via the nuclear factor- κ B pathway. *Oncol Rep* 45: 15, 2021.
- Ge S, Wu X, Xiong Y, Xie J, Liu F, Zhang W, Yang L, Zhang S, Lai L, Huang J, *et al*: HMGB1 inhibits HNF1A to modulate liver fibrogenesis via p65/miR-146b signaling. *DNA Cell Biol* 39: 1711-1722, 2020.
- Ge S, Zhang L, Xie J, Liu F, He J, He J, Wang X and Xiang T: MicroRNA-146b regulates hepatic stellate cell activation via targeting of KLF4. *Ann Hepatol* 15: 918-928, 2016.
- Kim YH, Choi CY, Lee SJ, Conti MA and Kim Y: Homeodomain-interacting protein kinases, a novel family of co-repressors for homeodomain transcription factors. *J Biol Chem* 273: 25875-25879, 1998.
- Meng L, Zhao X and Zhang H: HIPK1 interference attenuates inflammation and oxidative stress of acute lung injury via autophagy. *Med Sci Monit* 25: 827-835, 2019.
- Palkina N, Komina A, Aksenenko M, Moshev A, Savchenko A and Ruksha T: miR-204-5p and miR-3065-5p exert antitumor effects on melanoma cells. *Oncol Lett* 15: 8269-8280, 2018.
- Conte A and Pierantoni GM: Update on the regulation of HIPK1, HIPK2 and HIPK3 protein kinases by microRNAs. *MicroRNA* 7: 178-186, 2018.



This work is licensed under a Creative Commons Attribution-NonCommercial-NoDerivatives 4.0 International (CC BY-NC-ND 4.0) License.